Chair of Big Geospatial Data Management
TUM School of Engineering and Design
Technical University of Munich

Exploring Asteroids: A Survey

Semesterarbeit: Literature research and implementation of a relative position estimation for landing planning on an asteroid

Guerrero Hernández, Aníbal

October 30, 2024

Abstract - **Historically, exploration of asteroids has been reserved for larger missions due to the technological complexity and lack of available *a-priori* information, leading to a high risk of failure. Effective risk mitigation in such missions arises from adapting quickly to new and unforeseen conditions. This dynamic adaptation is driven by perception systems that require extensive data for accurate parameterization.**

This paper proposes a pipeline to generate synthetic image datasets by deforming base shape models, generating trajectories, and applying sensors. The proposed pipeline enhances the capabilities of the Outdoor Artificial Intelligent SYstems Simulator (OAISYS) by creating synthetic asteroid models. These models are used to generate RGB-Depth (RGB-D) images, masks, and six-dimensional (6D) pose data, which can train Convolutional Neural Network (CNN) models for detection, pose estimation, and tracking.

1. Introduction

Asteroid mining offers solutions to pressing challenges across domains by diversifying resource extraction beyond Earth, accessing Platinum Group Metals (PGMs) [1], Rare Earth Elements (REEs) [2], and water [3]. Not only would it ease the strain on Earth's resources, but also fuel aspirations for sustained space exploration, marking a pivotal step toward space industrialization. Beyond its economic promise, asteroid mining holds deep scientific significance, as it could shed light on solar system origins and planetary formation.

However, asteroid mining confronts significant technological barriers, requiring complex solutions for operation in space's harsh environment. Close-proximity navigation systems demand abundant *a-priori* information of the target [4], a challenge compounded by the scarcity of complete and precise image datasets. This lack of comprehensive datasets impedes the development of accurate models needed for effective navigation.

To address these challenges, CNN have emerged as a promising solution due to their adaptability to unknown and dynamic environments. However, for CNN to excel in detection, pose estimation, and tracking tasks, they necessitate substantial datasets for effective training. Compared to the 700,000 asteroids discovered [5], existing shape model catalogs such as the 3D Asteroid Catalogue, offer only 1,635 shape models, a negligible fraction of the asteroids discovered to date, with many models derived from lightcurve-inversion techniques, lacking the detail required for CNN-based approaches [6]. Assumptions like distant observation further limit the applicability of available datasets for tasks such as landing maneuvers.

This study aims to enhance the capabilities of the OAISYS to allow the generation of a comprehensive image dataset from synthetic asteroid shape models. Leveraging Blender's rendering engine, this initiative will create synthetic asteroid models, enabling RGB-D, mask, and 6D pose data collection. By bridging the gap between limited observational data and the needs of CNN-based algorithms, this effort lays the groundwork for advancements in autonomous navigation, detection, and pose estimation, benefiting asteroid mining and broader space exploration goals. The research ensured compatibility with existing Deep Learning (DL) frameworks to enhance training and evaluation processes for DL networks.

Research Trigger The purpose of this research lies in the recognition of the critical role of data in overcoming the challenges of asteroid mining. The scarcity of available data, particularly concerning three-dimensional (3D) asteroid models and asteroid image datasets, limits progress in mission planning and navigation. Synthetic data generation becomes a promising avenue to supplement sparse observational data, enabling the development of robust Machine Learning (ML) algorithms for asteroid exploration.

Research Questions To address these challenges, the following research questions guide this study:

Q1: What methods can be employed to generate a representative and realistic dataset of synthetic asteroid images suitable for training and evaluating DL networks?

Q2: What methodologies can be employed to validate the fidelity of the developed pipeline, ensuring the physical validity of the rotational movement of the asteroid?

Q3: How can the synthesis of real 3D asteroid data be optimized to generate a vast number of samples?

2. Related Work

Real asteroid imagery datasets provide insights into surface characteristics of asteroids. However, these often focus on a limited number of specific asteroids. In the context of ML models, these datasets could

lead to potential overfitting, resulting unusable in practice. As an example, Astrovision [7] offers a large-scale dataset featuring densely annotated images from observations collected throughout various deep space missions. The dataset consists of 110,000 densely annotated, real images of sixteen small bodies. Despite its richness, it lacks depth, 6D pose, mask information, and the dataset's narrow focus on only 16 asteroids limits its applicability to broader tasks.

The solution to the scarcity of real imagery datasets is to use real asteroid shape models derived from observational data and produce the images from these. Efforts such as the Database of Asteroid Models from Inversion Techniques (DAMIT) [8] aims to consolidate these shape models. At the time of this study, DAMIT contains around 200 shape models. However, shape models derived from lightcurve inversion techniques lack precision, lose most relevant geospatial information, and are scattered across various sources. Another example is the Planetary Data System (PDS) Small Bodies Node [9]. Similar to the DAMIT database, it is very limited in the total number of small bodies contemplated.

It is assumed that models have uniform, and constant density to model their volume. To do so, a Gaussian Quadrature over the surface is used to calculate the volume. This is a common assumption and implies that inner cavities, non-constant density distributions, and other structural irregularities are neglected, shifting the center of mass. The absence of *a-priori* information highlights the impossibility of knowing these internal structures.

The best database available is presented by 3D Asteroid Catalogue [6], an interactive catalogue that contains 1,635 shape models derived from lightcurve inversion, radar measurements, and spacecraft imagery, orbital and physical parameters, and current orbital position of known minor bodies. It is a compilation of multiple smaller datasets, where most of the radar-based models are taken from the JPL Asteroid RADAR Research page [10], and most of the lightcurve-inversion models are taken from the DAMIT database [8].

Compared to the 700,000 asteroids discovered at the time of writing this study, the 3D Asteroid Catalogue has a very small fraction of all asteroids identified. Additionally, the small sample of shape models available is in its majority, reconstructed from lightcurve-inversion models, which provides a low-detail shape estimation, inadequate for this study.

For this reason, it is reasonable to consider alternative approaches such as synthetic shape model generators. Specialized software like SurRender [11] and Planet and Asteroid Natural Scene Generation Utility (PANGU) [12] enables the generation of detailed 3D meshes based on procedural algorithms. However, these models may lack realism and depth compared to observational data, limiting their effectiveness in navigation applications.

Alternatively, AstroGen [13] presents a novel algorithm for generating highly detailed and physically realistic 3D meshes of small celestial bodies. AstroGen gains its realism from modeling surface details with physical equations derived from real-world asteroid data, overcoming traditional shape reconstruction methods' limitations. Nevertheless, requiring a high computational cost, leading to high execution times, and lacking relevant outputs such as depth maps and masks of the objects processed, as key to building CNN models, makes it an inadequate shape model generator for this study.

With regards to the asteroid, all trajectory simulations are taken without asteroid spin instabilities and all orbital families are contemplated. It assumes that observed synthetic asteroids have settled into a rotation around the principal axis of inertia due to energy dissipation over millennia, and direct, retrograde, and polar orbits are contemplated as a possibility when generating the asteroid trajectories.

3. Methodology

Given the limitations encountered with previous shape model generators, such as lack of realism, diversity, and relevant outputs essential for CNN models, OAISYS is chosen as the solution. OAISYS is a cutting-edge simulator designed to tackle the scarcity of high-quality synthetic data in planetary robotics [14]. Built upon Blender, it enables the creation of diverse planetary outdoor scenes with rich metadata, including semantic and instance annotations. By offering automated generation capabilities and high rendering quality, OAISYS facilitates the development of realistic datasets for various robotic tasks. Its modular design allows for easy customization, making it a versatile tool for researchers in planetary robotics and beyond.

System This study aims to expand on OAISYS as a foundational layer, enhancing its codebase to facilitate

the generation of synthetic asteroid datasets. The focus lies on creating a comprehensive database of synthetic asteroid models for training and evaluating DL networks. By simulating realistic asteroid environments, complete with deformed surfaces and dynamic trajectories, this research aims to bridge the gap between sparse observational data and the development of robust ML algorithms for asteroid exploration. The following requirements shall be met for a satisfactory outcome of this mission:

SR01: The OAISYS codebase shall be enhanced to support synthetic asteroid dataset generation.

SR02: A comprehensive database of synthetic asteroid shape models shall be created to generate rendered images, masks, and 6D poses for training and evaluating DL networks.

SR03: The research shall focus on simulating realistic asteroid environments with deformable surfaces and dynamic trajectories.

SR04: The generated outputs shall be usable with existing DL frameworks for training and evaluation.

Software Pipeline

The major steps of the dataset generation process are illustrated in Figure 1, serving as a top-level overview showing how it can be implemented for object detection, state estimation, and 3D model reconstruction CNN models.

The model-agnostic image generation pipeline consists of four parts. First, the base asteroid model is obtained and fed into the pipeline. Second, the synthetic asteroid models are generated by deforming the original base model and providing texture and lighting conditions. Then, trajectories are generated for each model. Lastly, the rendering process obtains mask, RGB-D, and 6D pose data. The different components in the pipeline are described in detail in the following subsections.

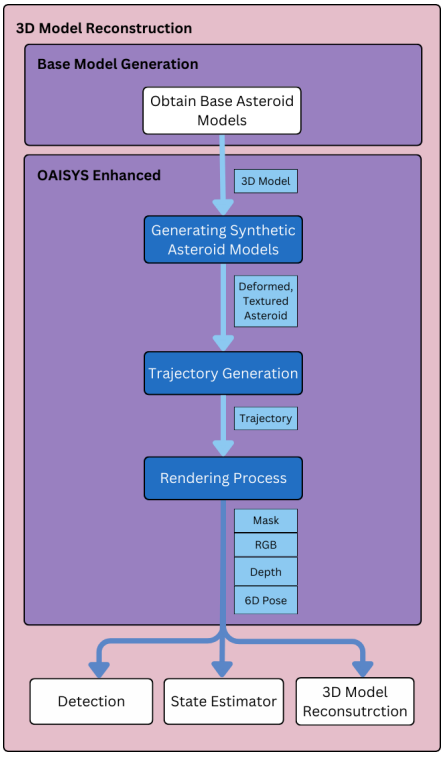

Figure 1 Overall schematic illustrating the software pipeline needed for image generation from synthetic asteroid models and how it is designed to be implemented into a larger navigation framework.

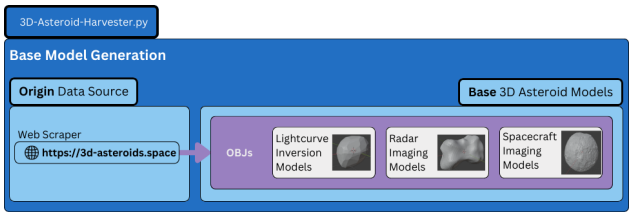

Figure 2 Schematic defining the origin data source used to collect the base asteroid models, and the different techniques used to reconstruct the Alias Wavefront Format (OBJ)s available.

Obtaining Base Asteroid Models

Base asteroid shape models are obtained from the 3D Asteroid Catalogue [6]. At the time of extraction, the database contains 1,635 asteroid models given in Stanford Triangle Format (PLY) and OBJ. This study only deals with OBJs, extracting the highest resolution option available for each asteroid. The OBJ datatype was selected for simplicity and consistency, as one format had to be chosen. While lightcurve inversion techniques dominate the creation of shape models, few asteroids have been observed using radar or have been visited by spacecraft. Notable examples include Eros [15], Itokawa and Vesta [16], each of which has yielded detailed shape models. Radar observations provide high-resolution data, allowing for the identification of surface features such as craters and ridges. Spacecraft missions, such as the NEAR Shoemaker mission to Eros and the Hayabusa mission to Itokawa [17], have provided unprecedented details into these asteroids' shapes and surface properties. However, these are a minority and would not be sufficient to construct significant CNN models with, as datasets should generally aim to handle large samples of more than 30,000+.

OAISYS Enhanced

Blender is selected as the rendering software. It is a powerful open-source, free 3D

modeling software, capable of creating and modifying 3D models and rendering images from 3D scenes through a Python API. Cinema4D has also been considered as an alternative, but Blender is selected for this study as it presents a superior user interface, texturing is a completely node-based system, is free, and requires less computational power [18].

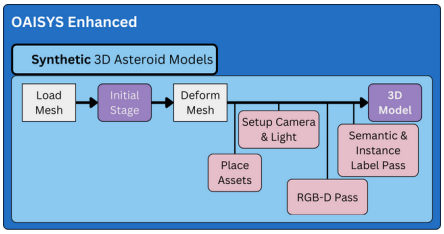

Figure 3 Schematic of how base asteroid 3D models are implemented into OAISYS, generated their trajectory, and rendered to produce RGB-D, 6D pose, and mask data.

Generation Synthetic Asteroid Models Due to the high availability of lower resolution shape models reconstructed with lightcurve techniques, OAISYS is implemented to derive synthetic shape models from these base shape models on a large scale. Normally, OAISYS generates an environment by modifying a main mesh known as the stage. However, this study implements a modification where an object (i.e. asteroid) directly serves as the base shape. The mesh of the shape model is loaded onto an empty stage, where it is deformed using a random noise out of a range such as Voronoi, Musgrave, random noise, and others. Deformation parameters are automatically adjusted after every batch iteration so that all synthetic shape models are different. Additionally, subsurface modifications are applied for fine-detail structures. A single configuration file governs all simulator parameters.

OAISYS can place objects known as assets, on top of another object's surface known as stage. In this study, no assets are placed on the synthetic shape model. Then, semantic and instance labels are rendered using the diffuse channel to address the drawbacks of object ID rendering, and semantic labels are encoded into RGB values for compatibility.

Moreover, lighting conditions are set with the respective module, altering parameters such as sun size and intensity. Then, target objects ensure that the camera viewpoint is focused, with adjustable constraints.

Trajectory Generation Once the synthetic shape models are processed, the performance of the algorithm is tested on image sequences representative of three different trajectories, typical of asteroids: direct (prograde), retrograde, and polar orbits. For direct orbits, the asteroid moves in the same direction as the Earth's rotation, whereas asteroids following a retrograde orbit move in the opposite direction to the planet's rotation, and polar orbits show a rotation over the poles. To simulate the different orbits, the sensor's position is adjusted relative to the origin. For example, by moving the sensor to the opposite side, an anticlockwise rotation (direct), can be perceived as clockwise (retrograde), and polar if moved at 90°.

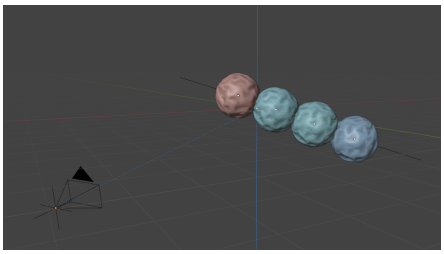

Figure 4 Schematic of a trajectory generated with a deformed sphere base shape model. The translation of each object is calculated by projecting a line between the initial position and the origin.

Generating a trajectory requires defining initial and final translations and rotations. As shown in Figure 4, the translation is simulated as a linear path, ensuring the shape model remains largely within the camera's field of view throughout the image sequence to be taken. Rotation parameters are initialized randomly, but the final rotation requires simulating a rotation around an axis. Asteroids spin around their principal axis of inertia due to energy dissipation, resulting in an oblate rotation pattern.

To calculate the principal axis of inertia, the center of mass and the moments of inertia around this center of mass are determined. Since the provided original reference frame does not correspond to the principal axes frame, the inertia matrix is non-diagonal. Therefore, the matrix is diagonalized to obtain the eigenvalues and eigenvectors. These eigenvalues form the diagonalized inertia matrix. Figure 5 illustrates the pipeline followed to calculate the rotation and translation generated for each new position.

In the theory of 3D rotation, Rodrigues' rotation formula is an efficient algorithm for rotating a vector in space given an axis and angle of rotation. The formula states that if $\mathbf{v}$ is a vector in $\mathbb{R}^3$ and $\mathbf{k}$ is a unit vector describing an axis of rotation about which $\mathbf{v}$ rotates by an angle θ, the rotated vector is given by:

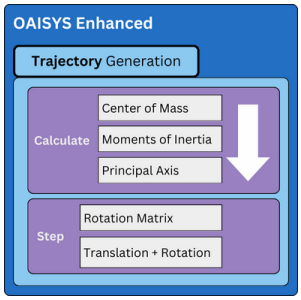

Figure 5 Schematic of how the trajectory is generated for each asteroid shape model processed.

$$\begin{aligned}\mathbf{v}_{\text{rot}} &= \mathbf{v}_{\parallel\text{rot}} + \mathbf{v}_{\perp\text{rot}} \\ &= \mathbf{v}_{\parallel} + \cos(\theta)\,\mathbf{v}_{\perp} + \sin(\theta)\mathbf{k}\times\mathbf{v},\end{aligned} \tag{1}$$

where the vector $\mathbf{v}$ is decomposed into components parallel and perpendicular to the axis $\mathbf{k}$ by using the dot and cross products respectively. Substituting $\mathbf{v}_{\perp} = \mathbf{v} - \mathbf{v}_{\parallel}$ in the last expression gives:

$$\mathbf{v}_{\text{rot}} = \mathbf{v}\cos\theta + (1-\cos\theta)(\mathbf{k}\cdot\mathbf{v})\mathbf{k} + \sin\theta(\mathbf{k}\times\mathbf{v}) \tag{2}$$

In matrix notation, the linear transformation on $\mathbf{v}$ is represented by $\mathbf{v} \mapsto \mathbf{k}\times\mathbf{v}$, the cross-product matrix $\mathbf{K}$. This matrix is skew-symmetric and given by:

$$\mathbf{K} = \begin{pmatrix} 0 & -k_z & k_y \\ k_z & 0 & -k_x \\ -k_y & k_x & 0 \end{pmatrix}, \tag{3}$$

where k_x, k_y, k_z are the components of the unit vector $\mathbf{k}$, corresponding to the principal axis of inertia of each base shape model. That is to say,

$$\mathbf{k}\times\mathbf{v} = \mathbf{K}\mathbf{v}, \qquad \mathbf{k}\times(\mathbf{k}\times\mathbf{v}) = \mathbf{K}(\mathbf{K}\mathbf{v}) = \mathbf{K}^2\mathbf{v}. \tag{4}$$

Substituting those terms in the previous equation gives

$$\mathbf{v}_{\text{rot}} = \mathbf{v} + (\sin\theta)\mathbf{K}\mathbf{v} + (1-\cos\theta)\mathbf{K}^2\mathbf{v}. \tag{5}$$

Collecting terms allows the compact expression

$$\mathbf{v}_{\mathbf{rot}} = \mathbf{R}\mathbf{v}, \tag{6}$$

where

$$\mathbf{R} = \mathbf{I} + (\sin\theta)\mathbf{K} + (1-\cos\theta)\mathbf{K}^2, \tag{7}$$

is the rotation matrix through an angle θ counterclockwise around the axis $\mathbf{k}$, and $\mathbf{I}$ is the 3×3 identity matrix. This matrix $\mathbf{R}$ is used to calculate the next position of the synthetic shape model.

The angle of rotation, θ, can be determined from the rotational velocity, ω_{rot}, and the time elapsed, t. The rotational velocity is given by:

$$\omega_{rot} = \frac{2\pi}{T_{rot}}, \tag{8}$$

where T_{rot} is the rotation period and corresponds to the time it takes for one complete rotation. The angle of rotation θ after a time period of t hours is:

$$\theta = \omega \cdot t, \tag{9}$$

To simulate the synthetic asteroid's motion, rotational data is obtained from Figure 6, which is generated based on the methodology outlined in [19], involving over 5000 asteroids. Over 95% of the rotational periods considered fall within the range of 2.55 to 49.29 hours, with a median rotational period of 8.12 hours. Moreover, the distribution of rotational periods is non-normal, as evidenced by the best-fit distribution being lognormal. For each new asteroid generated, rotational data is randomly sampled from within this range, with the corresponding mean and variance for the lognormal distribution found from the analysis.

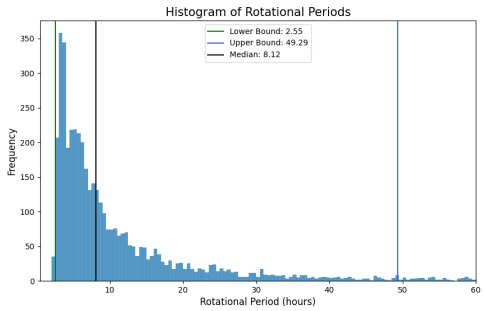

Figure 6 Distribution of periods derived from ATLAS [19] data, showing the median, lower, and upper bound.

Rendering Process Another advantage this simulation framework has over other relevant works is that it provides comprehensive instances for RGB-D images, 6D pose data, and mask instances for each synthetic shape model generated, as demonstrated in Figure 7. This extensive data collection is crucial for training various CNN models, as these outputs serve as the ground truth, thereby eliminating the need for extensive manual labeling.

The mask is a critical output for instance segmentation. The mask is a binary image that highlights the

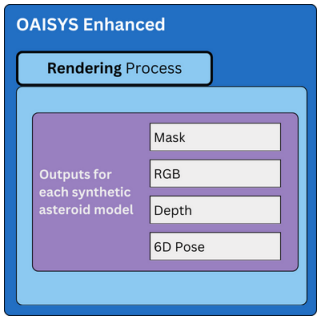

Figure 7 Schematic of all instances obtained for each new position generated.

presence of the object. As shown in Figure 8, the mask can be processed into a bounding box format compatible with the YOLO framework [20], essential for validating the performance of ML algorithms in object detection tasks. Labels for this format are exported with one text file per image, with one row per object as

$$(class, x_{center}, y_{center}, width, height) \quad (10)$$

format, where box coordinates must be normalized from zero to one, and class numbers should be zero-index.

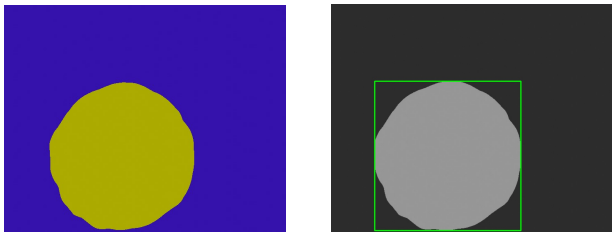

(a) Mask instance **(b)** Bounding Box

Figure 8 Sample of a YOLO format bounding box generated from an output mask instance.

The RGB and 6D pose data are indispensable for feature tracking as they combine color with geospatial information that details the object's position and orientation in space, using quaternion representation for rotation. The 6D pose throughout the trajectory is stored in one CSV file per shape model generated, with one row per position and a total number of rows corresponding to the samples generated per batch. The translation and rotation data are stored as

$$(x, y, z, q_w, q_x, q_y, q_z), \quad (11)$$

with the (x, y, z) as the translation components and (q_w, q_x, q_y, q_z) as the rotation quaternion components. Furthermore, the sensor's spatial information is stored in a separate file, following the same format.

One application of the annotated 6D pose is its use as the ground truth for tracking the object's movement across frames. Additionally, combining the depth output with the 6D pose enables the validation of a reconstructed 3D map of the sampled asteroid from monocular 2D observations.

4. Results

Synthetic Asteroid Generation As a form of visual representation, Figure 9 shows the result of processing a shape model through the enhanced OAISYS. The base shape model has no texture defined. However, the output processed a texture map and an environment, deformed the base shape model, and all semantic and instance passes are processed.

(a) Base asteroid model **(b)** Synthetic asteroid model

Figure 9 Outcome of processing asteroid 433 Eros base shape model with the enhanced OAISYS.

Trajectory Simulation Figure 10 illustrates an example trajectory generated with the enhanced OAISYS.

As depicted in Figure 10, the generated trajectory shows the translation and rotation of a synthetic shape model based on asteroid 433 Eros. It follows a direct trajectory. For each position provided in the sequence, a mask, an RGB image, a 6D pose, and a depth map are all stored.

Verification To ensure the accuracy of the generated trajectories, the calculations of the center of mass, moments of inertia, principal axes, and rotation matrices must be verified by comparing them to analytical solutions and referencing existing studies. A range of test cases is used to verify results, including a cube, cylinder, sphere, cone, and asteroid 433 Eros.

Calculating the center of mass is the point most prone to error due to the various methods available and the corresponding assumptions required for each. This

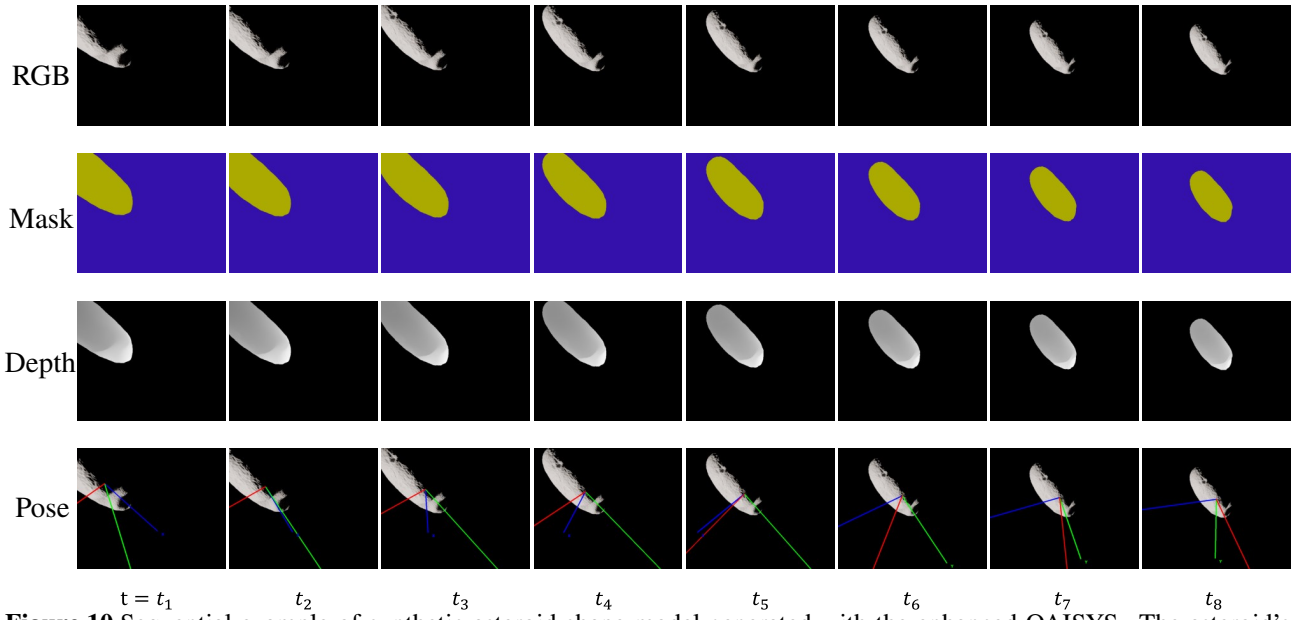

Figure 10 Sequential example of synthetic asteroid shape model generated with the enhanced OAISYS. The asteroid's direct orbit trajectory simulates a plausible rotation and translation based on the orbital parameters computed with data processed from Figure 6.

study assumes a uniform density throughout all volumes, allowing the use of Gaussian quadrature. Therefore, the following table compares the analytical solution for the center of mass of the object to the calculated solution. In the case of a cube, cylinder, sphere and cone, these values can be easily obtained using analytical solutions. However, the mass computation for the asteroid is verified using the approach of Chanut et al. [21], which calculates the polyhedral mass properties of 433 Eros using the fast and effective algorithm developed by Mirtich in C [22].

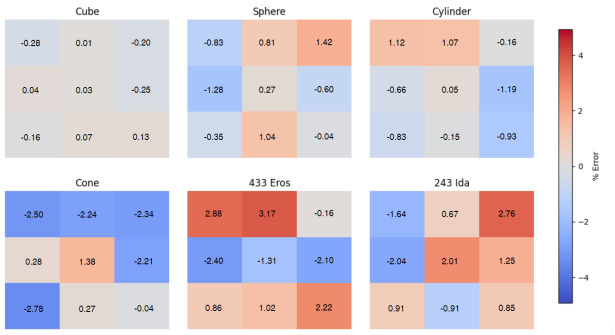

Figure 11 Error matrices in the moment of inertia calculations for sample objects and asteroid shape models.

The inertia matrix is verified against analytical solutions. As observed in Figure 11, certain irregularities can be observed as in the case of a sphere. This is due to the simplified mesh's inability to generate a perfectly round sphere. The phenomenon is also present in the cylinder and the cone. Due to the highly irregular shape of the asteroid shape models, these present the highest deviations from theoretical solutions provided in other studies, as deviations from the true center of mass and density distribution methods significantly impact the calculations.

Finally, the rotation matrix calculation error is the difference between the theoretical and calculated values and is represented in Figure 12, resulting in ~ 7%, due to a linear combination of all previous errors.

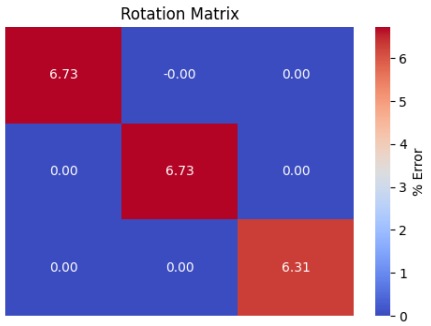

Figure 12 Error matrix in the calculation of the rotation matrix used in the trajectory generation for asteroid 433 Eros.

5. Conclusion & Outlook

The presented research serves as a foundational contribution to addressing the critical data limitations in utilizing CNN models for perception tasks within the context of asteroid mining. By generating a comprehensive image dataset from synthetic asteroid shape models using OAISYS, the research aims to pave the way for more robust ML algorithms applied to asteroid exploration.

Answering the first research question, this study developed a method involving the generation of synthetic asteroid images using OAISYS. This method includes the creation of RGB-D images, 6D pose data, masks, and depth images, which are essential for training and evaluating DL networks effectively.

Secondly, the research integrated three different orbital trajectories: direct, retrograde, and polar orbits into OAISYS. By adjusting the sensor's position, the rotational movement is consistently calculated, ensuring physical validity and accurate representation of real asteroid trajectories.

Finally, the study focused on leveraging the capabilities of OAISYS to create detailed and diverse shape models, optimizing the synthesis of real 3D asteroid data, and generating a vast number of samples. By using OAISYS, the synthesis process can generate numerous synthetic asteroid images with varying shapes and textures, which are crucial for building robust CNN models.

Outlook Looking ahead, future improvements could involve improving the physical realism in the synthetic shape models generated. While the current study focuses on generating synthetic asteroid images, future research could implement deformations through physically described equations that model craters and other irregularities present in asteroids. For instance, AstroGen [13], despite its high computational cost and limitations in output formats, demonstrates the potential for achieving high realism by modeling surface details with physical equations. Furthermore, incorporating more sophisticated surface texture models and realistic lighting conditions would improve resemblance to real-world observations.

Comparisons with observational data can provide valuable insights into the accuracy and fidelity of the synthetic datasets generated. By comparing synthetic data to actual observations, researchers can assess if they represent the physical characteristics and behaviors of real asteroids accurately.

Moreover, in the dataset generation process, a base shape model is assumed known, but with limited physical accuracy. The focus of this study is generating a pipeline for synthetic asteroid image datasets. Future studies may develop to improve the physical comparability of these models.

Lastly, this dataset generation model could be extrapolated to satellite imagery applications beyond. By leveraging the capabilities of OAISYS, synthetic datasets of satellite imagery could be generated to train ML algorithms for tasks such as satellite navigation or detection, broadening the applicability of the research.

References

[1] PV Sukumaran. Mining asteroid resources. *Geological Society of India*, 88(1):125–125, 2016.

[2] Claire L McLeod and Mark PS Krekeler. Sources of extraterrestrial rare earth elements: to the moon and beyond. *Resources*, 6(3):40, 2017.

[3] Conel M O'D Alexander, Kevin D McKeegan, and Kathrin Altwegg. Water reservoirs in small planetary bodies: meteorites, asteroids, and comets. *Space science reviews*, 214(1):36, 2018.

[4] Shota Takahashi and Daniel J Scheeres. Autonomous exploration of a small near-earth asteroid. *Journal of Guidance, Control, and Dynamics*, 44(4):701–718, 2021.

[5] Joseph A. Nuth, Brent Barbee, and Ronald Leung. Defending the earth from long-period comets and sneaky asteroids: Short term threat response requires long term preparation. *Journal of Space Safety Engineering*, 5(3):197–202, 2018.

[6] 3d asteroids catalogue. https://3d-asteroids.space/. Accessed: January 22, 2024.

[7] Travis Driver, Katherine A. Skinner, Mehregan Dor, and Panagiotis Tsiotras. Astrovision: Towards autonomous feature detection and description for missions to small bodies using deep learning. *Acta Astronautica*, 210:393–410, 2023.

[8] J. Durech, V. Sidorin, and M. Kaasalainen. DAMIT: a database of asteroid models. , 513:A46, April 2010.

[9] Planetary Data System (PDS) Small Bodies Node. Planetary Data System (PDS) Small Bodies Node. https://sbn.psi.edu/pds/. Accessed: April 22, 2024.

[10] Jet Propulsion Laboratory (JPL). JPL Asteroid RADAR Research. http://echo.jpl.nasa.gov/. Accessed: April 22, 2024.

[11] Roland Brochard, Jérémy Lebreton, Cyril Robin, Keyvan Kanani, Grégory Jonniaux, Aurore Masson, Noela Despré, and Ahmad Berjaoui. Scientific image rendering for space scenes with the surrender software. *arXiv preprint arXiv:1810.01423*, 2018.

[12] Pangu software. https://pangu.software/. Accessed: January 17, 2024.

[13] Xi-Zhi Li, René Weller, and Gabriel Zachmann. Astrogen – procedural generation of highly detailed asteroid models. In *2018 15th International Conference on Control, Automation, Robotics and Vision (ICARCV)*, pages 1771–1778, 2018.

[14] Marcus G. Müller, Maximilian Durner, Abel Gawel, Wolfgang Stürzl, Rudolph Triebel, and Roland Siegwart. A Photorealistic Terrain Simulation Pipeline for Unstructured Outdoor Environments. In *IEEE/RSJ International Conference on Intelligent Robots and Systems*, 2021.

[15] Changhao Chen, Bing Wang, Chris Xiaoxuan Lu, Niki Trigoni, and Andrew Markham. A survey on deep learning for localization and mapping: Towards the age of spatial machine intelligence, 2020.

[16] N. Mastrodemos, B. Rush, A. Vaughan, and W. Owen. Optical navigation for the dawn mission at vesta. *Advances in the Astronautical Sciences*, 140:1739–1754, 2011.

[17] Tatsuaki Hashimoto, Takashi Kubota, Jun'ichiro Kawaguchi, Masashi Uo, Kenichi Shirakawa, Takashi Kominato, and Hideo Morita. Vision-based guidance, navigation, and control of hayabusa spacecraft - lessons learned from real operation -. *IFAC Proceedings Volumes*, 43(15):259–264, 2010. 18th IFAC Symposium on Automatic Control in Aerospace.

[18] School of Motion. Blender vs. cinema 4d: A comparison. https://www.schoolofmotion.com/blog/blender-vs-cinema-4d. Accessed: April 22, 2024.

[19] J Ďurech, J Tonry, N Erasmus, L Denneau, AN Heinze, H Flewelling, and R Vančo. Asteroid models reconstructed from atlas photometry. *Astronomy & Astrophysics*, 643:A59, 2020.

[20] Joseph Redmon, Santosh Kumar Divvala, Ross B. Girshick, and Ali Farhadi. You only look once: Unified, real-time object detection. *CoRR*, abs/1506.02640, 2015.

[21] Thierry Chanut, O. Winter, and M. Tsuchida. 3d stability orbits close to 433 eros using an effective polyhedral model method. *Monthly Notices*

of the Royal Astronomical Society, 438:56–, 02 2014.

[22] Brian Mirtich. Fast and accurate computation of polyhedral mass properties. *Journal of Graphics Tools*, 1(2):31–50, 1996.